One-Bit Spectral-Correlation Algorithms

W. A. Gardner and R. S. Roberts

Abstract—**A technique that greatly simplifies the computational complexity of digital cyclic spectral analysis algorithms is presented. The technique, which is based on Bussgang's theorem, replaces complex multiplications in spectral correlation operations with simple sign-change and data-multiplexing operations. Moreover, the technique is applicable to both time- and frequency-averaging algorithms. A simulation study that compares the computed results obtained using the new technique with results from standard time- and frequency-averaging algorithms shows that the new technique is very promising, particularly for frequency-averaging algorithms.**

I. Introduction

Most modulated signals encountered in communications and telemetry systems exhibit cyclostationarity. A fundamental tool in the study and exploitation of cyclostationarity is the cyclic spectrum analyzer; that is, an instrument that computes the cyclic spectrum from signal measurements and graphs this function (its magnitude and/or phase) as the height of a surface above the bifrequency

Manuscript received May 25, 1991; revised April 20, 1992. This work was supported in part by a grant from ESL, Inc., with partial matching support from the California State MICRO Program.

W. A. Gardner is with the Signal Processing Group, Department of Electrical and Computer Engineering, University of California, Davis, CA 95616.

R. S. Roberts was with the Signal Processing Group, Department of Electrical and Computer Engineering, University of California, Davis, CA 95616. He is now with the Los Alamos National Laboratory, Los Alamos, NM 87545.

IEEE Log Number 9203368.

plane [1]–[2]. Since the cyclic spectrum is also a spectral correlation function, this instrument can also be called a spectral-correlation analyzer. The action of correlating all pairs of narrow-band spectral components throughout a relatively broad band is computationally intensive. Several approaches are available to perform the processing more quickly than is done by the most straight-forward methods. One approach is to exploit the structural properties of cyclic spectral analysis algorithms through partitioning and parallelizing the computations. This approach is considered in [3]–[7]. A second approach, which is considered in this correspondence, is to exploit the properties of the correlation operation that underlies cyclic spectral analysis.

Let us begin by describing the two basic methods of digital cyclic-spectral analysis: the time- and frequency-averaging methods [1]. For the sake of generality, we consider cyclic cross-spectral analysis of two complex-valued discrete-time signals $x(n)$ and $y(n)$ with unity time increment. For the time-averaging method, we have the cyclic spectrum estimate

$$S^{\alpha_0}_{xy_T}(n, f_0)_{\Delta t} \triangleq \frac{1}{T} \langle X_T(n, f_0 + \alpha_0/2)\, Y^*_T(n, f_0 - \alpha_0/2)\rangle_{\Delta t} \quad (1)$$

where $\langle \cdot \rangle_{\Delta t}$ denotes average over time t and Δt is the averaging time, and where the time-variant finite-time discrete Fourier transform $X_T(n, f)$ is given by

$$X_T(n, f) \triangleq \sum_{k=-N'/2}^{N'/2-1} a(k)x(k-n)e^{-j2\pi f(k-n)} \quad (2)$$

where $a(k)$ is a data-tapering window, and similarly for $Y_T(n, f)$. $X_T(n, f)$ can be interpreted as the down-converted output of a narrow-band-pass filter with bandwidth $\Delta f = 1/T$. The total amount of data used to compute a time-averaged estimate is $\Delta t = N$, and the amount of data used to compute the spectral components is $T = N'$. The frequency resolution of this algorithm is $\Delta f = 1/T = 1/N'$. For a statistically reliable estimate, it is necessary that $\Delta t \Delta f = N/N' \triangleq M \gg 1$ [1].

For a frequency-averaged estimate, we have

$$S^{\alpha_0}_{xy_{\Delta t}}(n, f_0)_{\Delta f} \triangleq \frac{1}{\Delta t} \langle X_{\Delta t}(n, f_0 + m/\Delta t + \alpha_0/2) \cdot Y^*_{\Delta t}(n, f_0 + m/\Delta t - \alpha_0/2)\rangle_{\Delta f} \quad (3)$$

where $\langle \cdot \rangle_{\Delta f}$ denotes average over the frequency index m; and Δf is the frequency-averaging bandwidth in units of m, and where the spectral components are given by

$$X_{\Delta t}(n, f) \triangleq \sum_{k=-N/2}^{N/2-1} a(k)x(k-n)e^{-j2\pi f(k-n)} \quad (4)$$

and similarly for $Y_{\Delta t}(n, f)$. The total amount of data used in this estimate is equal to the amount of data used to compute the spectral components $\Delta t = N$. The frequency resolution is some multiple of that of the transform: $\Delta f = M/N \triangleq 1/N'$. Again, for a statistically reliable measurement, it is required that $\Delta t \Delta f = M \gg 1$.

It can be seen that both methods compute the correlations (over time n or frequency f) of spectral components. Also, it can be shown [1] that the resolution of both these estimates in the cycle frequency parameter α is $\Delta\alpha = 1/\Delta t$. Thus, to cover the entire band of α, which ranges from -1 to $+1$ (for unity time increment), we must compute the cyclic spectrum for $2/\Delta\alpha = 2\Delta t$ many values of α. Also, since the resolution in the frequency parameter f is Δf, then in order to cover the entire band of f, which ranges from $-1/2$ to $+1/2$, and includes Δt frequency samples, we must compute each cyclic spectrum (for each value of α) $\Delta t/\Delta f$ times. Thus, we must compute $2(\Delta t)^2/\Delta f \triangleq K$ individual values of the cyclic spectrum, that is, $K = 2(\Delta t)^2/\Delta f$ individual correlations to cover the entire bifrequency plane. Useful values of Δf can range from 10^{-1} to 10^{-3}. Useful values of Δt range from 10^2 to 10^8 (with the largest values being required for low-SNR applications, such as spread-spectrum signals with SNR as low as -20 dB). Thus, K typically lies between 10^5 and 10^{19}. Clearly, the computational intensity of cyclic spectral analysis can be greatly improved by improving the efficiency of the correlation computations.

It has long been recognized that correlation computations involving real signals can be significantly simplified by clipping the amplitudes of one of the signals being correlated to the values ± 1, that is, by retaining only the signs of the amplitudes. With one of the signals clipped to ± 1, the multiplications in the correlation computation become sign-change operations. This approach has been used to advantage in several correlator structures (e.g., [8]). The advantages of such an approach are well known: less hardware, faster processing due to fewer logic delays, reduced storage requirements, and less data transfer between modules of implementing architectures.

The theoretical foundation for clipping one of the signals in a correlation computation is given by Bussgang's theorem [9]. In essence, Bussgang's theorem states that the cross correlation $R_{uv}(\tau)$ between two signals $u(t)$ and $v(t)$ has the same functional form in τ as the cross correlation $R_{uv'}(\tau)$ between $u(t)$ and $v'(t)$, where $v'(t)$ is derived from $v(t)$ by a nonlinear memoryless transformation—provided that $u(t)$ and $v(t)$ are stationary Gaussian processes. The two cross correlations differ by only a constant scaling factor. [Although the signals of primary interest in communications and telemetry are not Gaussian or stationary, the components $X_T(n, f)$ derived from them by band-pass filtering can be stationary and approximately Gaussian, and it is these components that we wish to correlate.] A particularly appropriate nonlinear memoryless transformation is the complex sign detector

$$\Phi[v] = \frac{1}{\sqrt{2}} [\text{sign}(\text{Re}[v]) + j\,\text{sign}(\text{Im}[v])]. \quad (5)$$

As just explained, this transformation can significantly reduce the computational complexity of a correlation operation. Thus, in the next section we use Bussgang's theorem to obtain approximations to the correlation operations used in the two cyclic spectral analysis algorithms (1) and (3). Then, in the final section, we present the results of simulations to illustrate the effects of the computational simplifications on the computed cyclic spectrum.

II. One-Bit Spectral Correlation Algorithms (OBSCA's)

Consider two jointly stationary zero-mean complex Gaussian processes $v(n)$ and $u(n)$. Let $v'(n)$ be obtained from $v(n)$ by any nonlinear memoryless transform $\Phi[\cdot]$ so that $v'(n) = \Phi[v(n)]$. In general, we have the identity

$$R_{uv}(0) \triangleq E\{u(n)v(n)^*\} \quad (6)$$

$$= \frac{E\{|v(n)|^2\}}{E\{v(n)\,v'(n)^*\}} E\{u(n)\,v'(n)^*\} \quad (7)$$

$$\triangleq \frac{R_v(0)}{R_{vv'}(0)} R_{uv'}(0) \quad (8)$$

$$= a_v R_{uv'}(0) \quad (9)$$

where

$$a_v = \frac{R_v(0)}{R_{vv'}(0)}. \quad (10)$$

Equation (7) is obtained by application of a version of Bussgang's theorem for complex-valued processes [9]. These results hold if the expectation operation $E\{\cdot\}$ is replaced by a time-averaging operation $\langle\cdot\rangle$ provided that the stationary joint fraction-of-time distribution of $u(n)$ and $v(n)$ (which is defined in [1]) is Gaussian even if $u(n)$ and $v(n)$ exhibit cyclostationarity (that is, they need not be purely stationary—see [1]).

It is desirable to use clipped data when computing $R_v(0)$ in the scale factor a_v in (10). To this end, we temporarily replace $u(n)$ with $v'(n)$ in (6)–(8) and solve for $R_v(0)$ to get

$$R_v(0) \cong \frac{R_{v'v}(0)}{R_{v'v'}(0)} R_{vv'}(0). \tag{11}$$

Since (7) is valid only for Gaussian processes $u(n)$ and $v(n)$, and since the temporary replacement $v'(n)$ for $u(n)$ is not Gaussian, then (10) is only an approximation. That this is a useful approximation is demonstrated with simulations in Section III. Substituting this approximation for $R_v(0)$ into (8) gives

$$R_{uv}(0) \cong \frac{R_{v'v}(0)}{R_{v'v'}(0)} R_{uv'}(0). \tag{12}$$

Now both the scale factor $R_{v'v}(0)/R_{v'v'}(0)$ and the correlation $R_{uv'}(0)$ can be computed using the same clipped data. The scale factor can be further simplified by observing that

$$R_{v'v'}(0) = \langle v'(n)\, v'(n)^*\rangle = \langle v_r'^{\,2}(n) + v_i'^{\,2}(n)\rangle. \tag{13}$$

Since $v_r'(n)$ and $v_i'(n)$ can take on values of only $\pm 1/\sqrt{2}$, then $R_{v'v'}(0) = 1$. Hence, the approximation (12) becomes

$$R_{uv}(0) \cong R_{v'v}(0)\, R_{uv'}(0). \tag{14}$$

By rotating the output of the complex sign detector by $\pi/4$ radians, further simplification in the correlation computation can be obtained [9]. Since the rotated output of the sign detector has one of four possible values, i.e., $1/\sqrt{2}$ times (1, 0), (0, 1), (−1, 0), or (0, −1), complex multiplications in the correlation computation are replaced by sign detection and multiplexing operations. Note that $R_{uv}(0)$ is unaffected by the rotation

$$\langle(\Phi[v(n)]\, e^{j\pi/4})\, v(n)^*\rangle\, \langle u(n)\,(\Phi[v(n)]\, e^{j\pi/4})^*\rangle$$
$$= R_{v'v}(0)\, e^{j\pi/4}\, R_{uv'}(0)\, e^{-j\pi/4} \tag{15}$$
$$= R_{v'v}(0)\, R_{uv'}(0). \tag{16}$$

In summary, by using this technique, complex multiplication in correlation computations is reduced to a multiplexing operation on the real and imaginary components of the input sequences.

To apply the preceding development to the computation of time-averaged estimates of the cyclic cross spectrum, let $u(n)$ and $v(n)$ be the complex-demodulate sequences $X_T(n, f_0 + \alpha_0/2)$ and $Y_T(n, f_0 - \alpha_0/2)$. For sufficiently large T, these will each be approximately stationary and Gaussian. However, they will not, in general, be independent and might not be approximately jointly Gaussian. Nevertheless, (14)–(16) suggest that the time-averaged cyclic cross spectrum (1) can be approximated by (ignoring constant scale factors)

$$S_{xy_T}^{\alpha_0}(n, f_0)_{\Delta t} \cong \frac{a(f_0 - \alpha_0/2)}{T} \langle X_T(n, f_0 + \alpha_0/2)$$
$$\cdot\, (\Phi(Y_T(n, f_0 - \alpha_0/2)]\, e^{j\pi/4})^*\rangle_{\Delta t} \tag{17}$$

where the scaling factor is

$$a(f_0 - \alpha_0/2) = \tfrac{1}{2}\langle\Phi[Y_T(n, f_0 - \alpha_0/2)]\, e^{j\pi/4}$$
$$\cdot\, Y_T^*(n, f_0 - \alpha_0/2)\rangle_{\Delta t}. \tag{18}$$

To obtain a similar approximation for the frequency-averaged estimates of the cross-cyclic spectrum, we observe that for sufficiently large Δt and small Δf, the spectral components $u(m) \triangleq X_T(n, f_0 + m/\Delta t + \alpha_0/2)$ and $v(m) \triangleq Y_T(n, f_0 + m/\Delta t - \alpha_0/2)$ (in which m is a frequency index) that are correlated in (3) are each approximately statistically stationary in m throughout the averaging band of width Δf. They are also each approximately Gaussian (although they might not be approximately jointly Gaussian). Again, (14)–(16), with $u(n)$ and $v(n)$ there replaced by $u(m)$ and $v(m)$ here, suggest that the frequency-averaged cyclic cross spectrum (3) can be approximated by

$$S_{xy_{\Delta t}}^{\alpha_0}(n, f_0)_{\Delta f} = \frac{b(f_0 - \alpha_0/2)}{\Delta t} \langle X_{\Delta t}(n, f_0 + m/\Delta t + \alpha_0/2)$$
$$\cdot\, (\Phi[Y_{\Delta t}(n, f_0 + m/\Delta t - \alpha_0/2)]\, e^{j\pi/4})^*\rangle_{\Delta f} \tag{19}$$

where the scaling factor is

$$b(f_0 - \alpha_0/2) = \tfrac{1}{2}\langle\Phi[Y_{\Delta t}(n, f_0 + m/\Delta t - \alpha_0/2)]\, e^{j\pi/4}$$
$$\cdot\, Y_{\Delta t}^*(n, f_0 + m/\Delta t - \alpha_0/2)\rangle_{\Delta f}. \tag{20}$$

Referring to (17) and (19), it is noted that the same sequences $u(n) = Y_T(n, f_0 - \alpha_0/2)$ or $u(n) = Y_{\Delta t}(n, f_0 + m/\Delta t - \alpha_0/2)$ for each of these methods is used to compute all point estimates with coordinates f_0 and α_0 satisfying $f_0 - \alpha_0/2 =$ constant. The locus of these estimates is a diagonal line in the bifrequency plane. It can be seen from (18) and (20) that the scaling factors in (17) and (19) are the same along each such diagonal. Since only $1/\Delta f$ such diagonals are needed to cover the plane (since the resolution in f is Δf, then we can increment f_0 by the amount Δf), then only $1/\Delta f$ scale factors need to be computed for the entire plane.

The computationally simplified algorithms (17)–(18) and (19)–(20) are called one-bit spectral correlation algorithms (OBSCA's). The OBSCA technique has several advantages when applied to the very-large-scale-integration implementation of cyclic spectrum analyzers. Foremost is the hardware simplification gained by replacing complex multipliers used in the spectral correlation operation with OBSCA arithmetic units. The hardware simplification is especially apparent in architectures designed to compute the frequency-averaged cyclic cross periodogram. Since the OBSCA technique requires only the sign bit from the real and imaginary parts of spectral data, data storage and movement requirements are greatly reduced. Reduced data storage, coupled with reduced arithmetic-logic-unit (ALU) complexity and two-bit-wide data buses, allow for signal processors with large on-chip data caches. As a result of having large amounts of data on chip, the efficiency of the ALU increases along with the speed of the spectral correlation computation.

III. Simulation Study

To assess the performance of the OBSCA's, a series of simulations were performed. In these simulations, the input signal consists of either 8192 or 65 536 time samples of a single binary phase-shift-keyed (BPSK) signal in white Gaussian noise with 0dB SNR in the band of the signal. The center frequency of the signal is 0.3125, and the keying rate is 0.0625. Simulations were performed to estimate the cyclic spectrum along the lines $\alpha = 0.0625$ and $\alpha = 0.625$. These positions correspond to the keying-rate feature and carrier feature of the BPSK signal [1]. The frequency resolution of all estimates is $\Delta f = 1/32$ and the time-frequency resolution product is either $\Delta t \Delta f = 256$ or $\Delta t \Delta f = 2048$. Figs. 1–4 show plots of magnitude versus frequency on linear scales for particular values

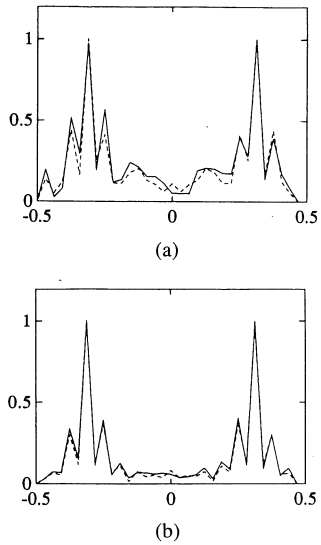

Fig. 1. (a) Broken curve: time-averaged estimate along $\alpha = 0.0625$ with $\Delta t \Delta f = 256$; peak value = 0.50. Continuous curve: OBSCA time-averaged estimate along $\alpha = 0.0625$ with $\Delta t \Delta f = 256$; peak value = 0.30; and (b) broken curve: time-averaged estimate along $\alpha = 0.0625$ with $\Delta t \Delta f = 2048$; peak value = 0.63. Continuous curve: OBSCA time-averaged estimate along $\alpha = 0.0625$ with $\Delta t \Delta f = 2048$; peak value = 0.73.

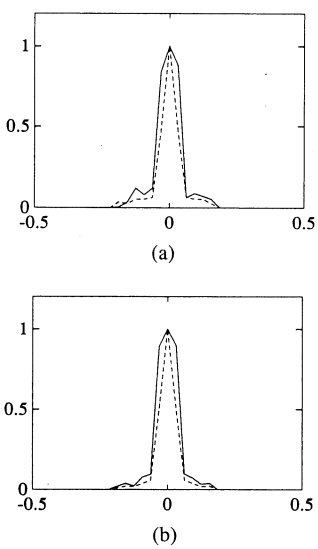

Fig. 2. (a) Broken curve: time-averaged estimate along $\alpha = 0.625$ with $\Delta t \Delta f = 256$; peak value = 1.53. Continuous curve: OBSCA time-averaged estimate along $\alpha = 0.625$ with $\Delta t \Delta f = 256$; peak value = 0.53; and (b) broken curve: time-averaged estimate along $\alpha = 0.625$ with $\Delta t \Delta f = 2048$; peak value = 1.67. Continuous curve: OBSCA time-averaged estimate along $\alpha = 0.625$ with $\Delta t \Delta f = 2048$; peak value = 1.15.

of cycle frequency. Some figures exhibit extended regions of zero amplitude (cf. Figs. 2 and 4). These regions are beyond the region of support of the cyclic spectrum. All figures are scaled so that the peak value is unity. The figure caption indicates the peak value of the data set before scaling.

The broken curve in Fig. 1(a) is the time-averaged estimate with $\Delta t \Delta f = 256$ for $\alpha = 0.0625$, which is the keying rate. The continuous curve in Fig. 1(a) is the same estimate using the OBSCA technique. Fig. 1(b) is the same, except $\Delta t \Delta f = 2048$. (In all figures, the broken curves are either standard time- or frequency-averaged estimates and the continuous curves are either time- or frequency-averaged estimates using the OBSCA.) Fig. 2(a) and (b) shows time-averaged estimates for $\alpha = 0.625$, which is the doubled carrier frequency. Fig. 3(a) and (b) shows frequency-averaged estimates for $\alpha = 0.0625$, and Fig. 4(a) and (b) shows frequency-averaged estimates for 0.625. For clarity in the graphics, Figs. 1–4 plot every 16th point of the 8192 frequency points or every 128th point of the 65 536 frequency points.

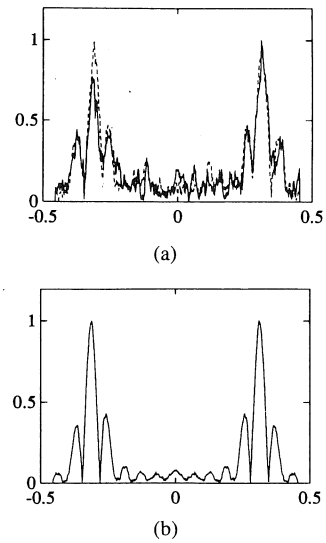

Fig. 3. (a) Broken curve: frequency-averaged estimate along $\alpha = 0.0625$ with $\Delta t \Delta f = 256$; peak value = 0.65. Continuous curve: OBSCA frequency-averaged estimate along $\alpha = 0.0625$ with $\Delta t \Delta f = 256$; peak value = 0.52 (every 16th point of the estimate is plotted); and (b) broken curve: frequency-averaged estimate along $\alpha = 0.0625$ with $\Delta t \Delta f = 2048$; peak value = 0.75. Continuous curve: OBSCA frequency-averaged estimate along $\alpha = 0.0625$ with $\Delta t \Delta f = 2048$; peak value = 1.50 (every 128th point of the estimate is plotted).

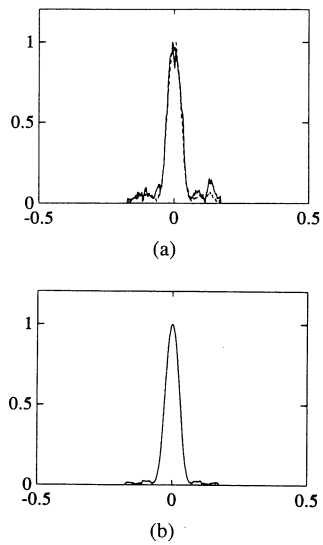

Fig. 4. (a) Broken curve: frequency-averaged estimate along $\alpha = 0.625$ with $\Delta t \Delta f = 256$; peak value = 1.76. Continuous curve: OBSCA frequency-averaged estimate along $\alpha = 0.625$ with $\Delta t \Delta f = 256$; peak value = 1.07 (every 16th point of the estimate is plotted); and (b) broken curve: frequency-averaged estimate along $\alpha = 0.625$ with $\Delta t \Delta f = 2048$; peak value = 1.89. Continuous curve: OBSCA frequency-averaged estimate along $\alpha = 0.625$ with $\Delta t \Delta f = 2048$; peak value = 3.77 (every 128th point of the estimate is plotted).

It can be seen from Figs. 1 and 2 that the time-averaged estimates produced by the OBSCA are as good as those produced by the corresponding conventional algorithm for the purpose of detection of the presence of a feature. However, for accurate measurement of the shape of a feature, the OBSCA might have some draw-

backs since its measurements do not exactly match those of the conventional algorithm, which is known to produce consistent estimates. On the other hand, it can be seen from Figs. 3 and 4 that the frequency-averaged estimates produced by the OBSCA very closely match those produced by the corresponding conventional algorithm. This is so for 8192 time samples and, for 65 536 time samples, there is no discernible difference: one measurement curve lies exactly on top of the other. This is an especially positive result since the OBSCA is particularly attractive from an implementation standpoint for the frequency-averaged estimates.

IV. Conclusions

A one-bit (the sign-bit) multiplier is introduced into the correlation operation in each of the two basic algorithms for cyclic spectral analysis (or spectral correlation analysis). For the algorithm that produces frequency-averaged estimates, this results in substantial hardware simplifications while producing very accurate estimates of the cyclic spectrum. For the algorithm that produces time-averaged estimates, the hardware simplifications are more moderate and some accuracy in the estimates is sacrificed. In conclusion, the one-bit spectral-correlation algorithm for producing frequency-averaged estimates shows great promise for the realization of practical spectral-correlation analyzers.

References

[1] W. A. Gardner, *Statistical Spectral Analysis: A Nonprobabilistic Theory*. Englewood Cliffs, NJ: Prentice-Hall, 1987.

[2] W. A. Gardner, "Exploitation of spectral redundancy in cyclostationary signals," *IEEE Signal Processing Mag.*, pp. 14–36, Apr. 1991.

[3] W. A. Brown, "On the theory of cyclostationary signals," Ph.D. dissertation, Dep. Elec. Comput. Eng., Univ. California, Davis, 1987.

[4] W. A. Brown and H. H. Loomis, Jr., "Digital implementations of spectral correlation analyzers," in *Proc. Fourth Annual ASSP Workshop Spectrum Estimation Modeling*, Minneapolis, Aug. 1988, pp. 264–270.

[5] R. S. Roberts, "Architectures for digital cyclic spectral analysis," Ph.D. dissertation, Dep. Elec. Comput. Eng., Univ. of California, Davis, 1989.

[6] R. S. Roberts, W. A. Brown, and H. H. Loomis, Jr., "Computationally efficient algorithms for cyclic spectral analysis," *IEEE Signal Processing Mag.*, pp. 38–49, Apr. 1991.

[7] W. A. Brown and H. H. Loomis, Jr., "Digital implementations of spectral correlation analyzers," *IEEE Trans. Signal Processing*, to be published.

[8] A. Gupta and W. Birkemeier, "Estimation of a quadrature cross-correlation detector by analog, polarity-coincidence and relay methods," *IEEE Trans. Informat. Theory*, pp. 859–865, Nov. 1984.

[9] G. Jacovitti *et al.*, "Methods of estimating the autocorrelation function of complex Gaussian stationary processes," *IEEE Trans. Acoust., Speech, Signal Processing*, pp. 1126–1138, Aug. 1987.